

# Path-integral calculation of the fourth virial coefficient of helium isotopes

Giovanni Garberoglio<sup>1, 2, a)</sup> and Allan H. Harvey<sup>3, b)</sup>

<sup>1)</sup>*European Centre for Theoretical Studies in Nuclear Physics and Related Areas (FBK-ECT\*), Trento, I-38123, Italy*

<sup>2)</sup>*Trento Institute for Fundamental Physics and Applications (TIFPA-INFN), Trento, I-38123, Italy*

<sup>3)</sup>*Applied Chemicals and Materials Division, National Institute of Standards and Technology, Boulder, CO 80305, USA*

(Dated: 23 December 2024)

We use the path-integral Monte Carlo (PIMC) method and state-of-the-art two-body and three-body potentials to calculate the fourth virial coefficients  $D(T)$  of  $^4\text{He}$  and  $^3\text{He}$  as functions of temperature from 2.6 K to 2000 K. We derive expressions for the contributions of exchange effects due to the bosonic or fermionic nature of the helium isotope; these effects have been omitted from previous calculations. The exchange effects are relatively insignificant for  $^4\text{He}$  at the temperatures considered, but for  $^3\text{He}$  they are necessary for quantitative accuracy below about 4 K. Our results are consistent with previous theoretical work (and with some of the limited and scattered experimental data) for  $^4\text{He}$ ; for  $^3\text{He}$  there are no experimental values and this work provides the first values of  $D(T)$  calculated at this level. The uncertainty of the results depends on the statistical uncertainty of the PIMC calculation, the estimated effect of omitting four-body and higher terms in the potential energy, and the uncertainty contribution propagated from the uncertainty of the potentials. At low temperatures, the uncertainty is dominated by the statistical uncertainty of the PIMC calculations, while at high temperatures the uncertainties related to the three-body potential and to omitted higher-order contributions become dominant.

## I. INTRODUCTION

State-of-the-art metrology for temperature and pressure increasingly relies on properties of helium calculated from first principles. Helium is unique among noble gases in that its small number of electrons allows the pair interaction between atoms to be computed almost exactly; the non-additive three-body interaction can also be calculated accurately. Statistical mechanics (sometimes along with other atomic properties such as the polarizability that can also be accurately calculated) can then provide properties of helium gas more accurately than they can be measured. Examples of this approach include modern acoustic gas thermometry,<sup>1</sup> dielectric-constant gas thermometry,<sup>2</sup> refractive-index gas thermometry,<sup>3</sup> and the recent development of a primary pressure standard based on dielectric measurements of helium.<sup>4</sup>

Helium also has the advantage of remaining in the gaseous state to low temperatures, making it the only feasible gas for metrology below about 25 K. Most metrology uses natural helium which is predominantly the  $^4\text{He}$  isotope, but the rare isotope  $^3\text{He}$  may be used at very low temperatures due to its even lower liquefaction temperatures.

The most important quantities in these applications are the virial coefficients that define the equation of state of a gas of molar density  $\rho$  at temperature  $T$  in an expansion around the ideal-gas (zero-density) limit,

$$\frac{p}{\rho RT} = 1 + B(T)\rho + C(T)\rho^2 + D(T)\rho^3 + \dots, \quad (1)$$

where  $p$  is the pressure and  $R$  is the molar gas constant. The second virial coefficient  $B(T)$  depends on the interaction be-

tween two molecules, the third virial coefficient  $C(T)$  depends on interactions among three molecules, and so on. While for many substances the most accurate values of these coefficients are those obtained from careful analysis of density data, for small molecules first-principles calculations may be able to obtain smaller uncertainties than experiment. Calculation of virial coefficients from intermolecular potentials will be described in the next section; here we note that, due to the low mass of helium, classical virial coefficient calculations are insufficient and quantum effects must be included (including exchange effects at very low temperatures).

For helium, in 2012 Cencek *et al.*<sup>5</sup> reported values of  $B(T)$  of unprecedented accuracy calculated from a pair potential that incorporated higher-order effects (adiabatic correction to the Born-Oppenheimer approximation, relativistic effects, quantum electrodynamics). The potential was further improved in 2017 by Przybytek *et al.*,<sup>6</sup> and still further in 2020 by Czachorowski *et al.*<sup>7</sup> The 2020 work reports  $B(T)$  for both  $^4\text{He}$  and  $^3\text{He}$  with uncertainties 5-10 times smaller than the uncertainties obtained by Cencek *et al.*<sup>5</sup> This accuracy results both from the highly accurate pair potential and from the fact that an exact quantum calculation of  $B(T)$  is possible via a phase-shift method.<sup>8</sup>

For the third virial coefficient  $C(T)$ , no exact solution is known, but the fully quantum result can be approached numerically with the path-integral Monte Carlo (PIMC) method. The most accurate first-principles values of  $C(T)$  come from Garberoglio *et al.*,<sup>9-12</sup> who used the same pair potential as Cencek *et al.*<sup>5</sup> and the three-body potential reported by Cencek *et al.*<sup>13</sup> They found that it was necessary to account for non-Boltzmann statistics (exchange) below approximately 5 K for  $^4\text{He}$  and 6 K for  $^3\text{He}$ .<sup>9,10</sup> They also estimated the uncertainty of  $C(T)$ , which primarily arose from the uncertainty of the three-body potential and (at low temperatures) from the statistical uncertainty of the PIMC calculations. These results,

<sup>a)</sup>Electronic mail: garberoglio@ectstar.eu

<sup>b)</sup>Electronic mail: allan.harvey@nist.gov

at least in the Boltzmann case, were confirmed independently by the group of Kofke.<sup>14,15</sup>

For many purposes, knowledge of  $B(T)$  and  $C(T)$  is sufficient. However, at higher pressures, terms containing  $D(T)$  become significant. Such terms contributed to the uncertainty budgets of a recent pressure standard<sup>4</sup> and recent single-pressure refractive-index gas thermometry measurements at cryogenic temperatures.<sup>16</sup> Efforts to calculate  $D(T)$  for helium that include quantum effects have been rare. Garberoglio performed approximate calculations above 100 K using a centroid-based method.<sup>17</sup> The group of Kofke came the closest to a rigorous calculation,<sup>14,15</sup> employing PIMC (considering only Boltzmann statistics) to calculate  $D(T)$  for  ${}^4\text{He}$  from 2.6 K to 1000 K based on accurate pair<sup>5</sup> and three-body<sup>13</sup> potentials. However, no uncertainties were reported apart from the statistical uncertainty of the PIMC calculations, and the results of Garberoglio and Harvey<sup>9,10</sup> for  $C(T)$  suggest that the neglect of exchange effects will cause these Boltzmann results to be in error at the lowest temperatures.

In this work, we use state-of-the-art pair<sup>7</sup> and three-body<sup>13</sup> potentials to compute  $D(T)$ , fully incorporating exchange effects in our PIMC calculations. We also provide the first rigorous calculations of  $D(T)$  for  ${}^3\text{He}$ , and provide uncertainty estimates that include not only statistical uncertainty but also the contribution of uncertainties in the potentials.

## II. VIRIAL COEFFICIENTS AND EXCHANGE EFFECTS

In Eq. (1), the virial coefficients are known from statistical mechanics<sup>8,18,19</sup> and depend on the  $N$ -body partition functions  $Q_N(V, T)$  according to

$$\frac{B(T)}{N_A} = -\frac{Z_2 - Z_1^2}{2V} \quad (2)$$

$$\frac{C(T)}{N_A^2} = \frac{(Z_2 - Z_1^2)^2}{V^2} - \frac{Z_3 - 3Z_2Z_1 + 2Z_1^3}{3V} \quad (3)$$

$$\frac{D(T)}{N_A^3} = -\frac{Z_4 - 4Z_3Z_1 - 3Z_2^2 + 12Z_2Z_1^2 - 6Z_1^4}{8V} + \frac{3(Z_2 - Z_1^2)(Z_3 - 3Z_2Z_1 + 2Z_1^3)}{2V^2} - \frac{5(Z_2 - Z_1^2)^3}{2V^3}, \quad (4)$$

where  $N_A$  is the Avogadro constant and the auxiliary functions  $Z_N$  are defined as

$$\frac{Z_N}{N!} = \frac{Q_N(V, T)}{Q_1(V, T)^N} \quad (5)$$

The appearance of powers of the Avogadro constant in the definition of virial coefficients is due to the fact that Eq. (1) has been written in terms of molar quantities, as the virial coefficients are usually reported; for the sake of conciseness we will omit these factors in subsequent formulae for  $B$ ,  $C$ , and  $D$  with the understanding that they must be applied as in Eqs. (2)-(4) to produce the virial coefficients in molar units.

In general, the partition functions  $Q_N(V, T)$  are given by

$$Q_N(V, T) = \sum_i' \langle i | e^{-\beta H_N} | i \rangle \quad (6)$$

$$= \frac{1}{N!} \sum_{i, \sigma} \langle i | e^{-\beta H_N} P_\sigma | i \rangle, \quad (7)$$

where  $H_N = K_N + V_N$  is the Hamiltonian of an  $N$  particle system, where  $K_N$  the total kinetic energy and  $V_N$  the total potential energy of  $N$  particles, respectively. The non-additive part of the  $N$  body potential will be denoted  $u_N$  instead, so that  $V_2 = u_2$ ,  $V_3 = u_3 + \sum_{i < j}^3 u_2(i, j)$ , and  $V_4 = u_4 + \sum_{i < j < k}^4 u_3(i, j, k) + \sum_{i < j}^4 u_2(i, j)$ . The primed sum in Eq. (6) is over the many-body states  $|i\rangle$  with the correct symmetry upon particle exchange in the case of bosonic or fermionic particles. Equation (7) is an equivalent expression for the partition function, where the sum is over a complete set of many-body states irrespective of the symmetry upon exchange and  $\sigma$  are the permutations of  $N$  objects.  $P_\sigma$  is an operator performing the permutation in the Hilbert space, which is multiplied by the sign of the permutation in the case of fermions.

In general, not all the degrees of freedom of the state of the system that we have denoted by  $|i\rangle$  appear in the Hamiltonian  $H_N$ . We will denote by  $x$  the set of the degrees of freedom appearing in  $H_N$  (atomic coordinates, in our case) and with  $s$  the other ones (nuclear spins), so that we can write  $|i\rangle = |s\rangle|x\rangle$ .

In the following we will use Eqs. (2–7) to derive explicit expressions for the quantum statistical contributions to virial coefficients that apply at low temperatures. The analogous formula for the second virial coefficient has been known for a long time,<sup>20</sup> but its derivation will be useful to fix the notation used in the remainder of the paper. In the case of the third virial coefficient, we will provide derivation of the formulae reported in Refs. 9 and 10. The fourth virial coefficient is newly developed in this work.

### A. The second virial coefficient

Let us begin with the calculation of  $Q_2$ . There is only one (trivial) permutation appearing in Eq. (7), and we will denote it by  $P$ . Performing the sum over the states we obtain<sup>9</sup>

$$Q_2(V, T) = n \frac{V}{\Lambda^3}, \quad (8)$$

where  $n$  is the number of internal states of the atoms we are considering and  $\Lambda = h/\sqrt{2\pi m k_B T}$  is the de Broglie thermal wavelength of a particle of mass  $m$ , which here can be either the mass of the  ${}^4\text{He}$  atom or the mass of the  ${}^3\text{He}$  atom. For helium isotopologues,  $n = 2I + 1$  where  $I$  is the nuclear spin state;  $I = 0$  for  ${}^4\text{He}$  (so  $n = 1$ ) and  $I = 1/2$  for  ${}^3\text{He}$  ( $n = 2$ ). Notice that  $Z_1 = V$ .

In the evaluation of  $Q_2(V, T)$ , we must consider two permutations. The first one is the identity, which we will denote by  $P^c$ , whereas the other exchanges the labels of the two particles and we will denote it by  $P^l$ . The latter permutation is odd, and hence its contribution is weighted with a + sign in the case of bosons and a – sign in the case of fermions. We have

$$Q_2(V, T) = \frac{1}{2} \left[ \left( \sum_{s_1, s_2} \langle s_1, s_2 | P^{\cdot} | s_1, s_2 \rangle \right) \langle x_1, x_2 | e^{-\beta H_2} P^{\cdot} | x_1, x_2 \rangle \pm \left( \sum_{s_1, s_2} \langle s_1, s_2 | P^{\dagger} | s_1, s_2 \rangle \right) \langle x_1, x_2 | e^{-\beta H_2} P^{\dagger} | x_1, x_2 \rangle \right] \\ = \frac{1}{2} \left[ n^2 \langle x_1, x_2 | e^{-\beta H_2} P^{\cdot} | x_1, x_2 \rangle \pm n \langle x_1, x_2 | e^{-\beta H_2} P^{\dagger} | x_1, x_2 \rangle \right], \quad (9)$$

$$\equiv \frac{1}{2} \left[ n^2 Q_2^{\cdot}(V, T) \pm n Q_2^{\dagger}(V, T) \right], \quad (10)$$

where the last equation defines the Boltzmann and exchanged partition function, given by  $Q_2^{\cdot}$  and  $Q_2^{\dagger}$ , respectively. The factor  $n^2$  in front of  $Q_2^{\cdot}$  comes from the fact that  $P^{\cdot}$  is the identity and the weight  $n$  in front of  $Q_2^{\dagger}$  from the fact that

$$\sum_{s_1, s_2} \langle s_1, s_2 | P^{\dagger} | s_1, s_2 \rangle = \sum_{s_1, s_2} \langle s_1, s_2 | s_2, s_1 \rangle = \sum_{s_1, s_2} (\delta_{s_1, s_2})^2 = n.$$

As detailed in our previous work,<sup>9,11</sup> the Boltzmann partition function can be evaluated in the path-integral framework and its final expression is equivalent to the partition function of a system where each of the two quantum particles is replaced by a classical ring polymer with  $P$  monomers (the equivalence being exact in the  $P \rightarrow \infty$  limit). The theory describes the form of the probability for a ring-polymer configuration  $F(\Delta \mathbf{r}_1, \dots, \Delta \mathbf{r}_{P-1}; m, P, T)$ ,<sup>9</sup> where  $\Delta \mathbf{r}_i = \mathbf{r}_{i+1} - \mathbf{r}_i$  is the separation between the position of a bead and the subsequent one. Since the distribution  $F$  is translationally invariant, it is convenient to assume that  $\mathbf{r}_1$  is the null vector. Notice that the distance between the last bead and the first one is given by the condition of having a closed polymer, hence  $\mathbf{r}_P - \mathbf{r}_1 = -\sum_{i=1}^{P-1} \Delta \mathbf{r}_i$ .

Analogously, the exchanged partition function is equivalent to the partition function of a *single* ring polymer of  $2P$  monomers. Finally, from Eqs. (10), (5), and (2), one obtains, for any value of the nuclear spin  $I$ ,

$$B(T) = B_{\text{Boltz}}(T) + \frac{(-1)^{2I}}{2I+1} B_{\text{xc}}(T) \quad (11)$$

$$B_{\text{Boltz}}(T) = -\frac{1}{2V} (Z_2^{\cdot} - V^2) \quad (12)$$

$$B_{\text{xc}}(T) = -\frac{Z_2^{\dagger}}{2V} \quad (13)$$

where, denoting by  $\overline{V_2^{\cdot}}$  and  $\overline{V_2^{\dagger}}$  the potential energies of the equivalent classical systems for the identity and the swap permutations, one has

$$\frac{Z_2^{\cdot}}{V} = \int d\mathbf{r} \left\langle e^{-\beta \overline{V_2^{\cdot}}} \right\rangle \quad (14)$$

$$\frac{Z_2^{\dagger}}{V} = \frac{\Lambda^3}{2^{3/2}} \left\langle e^{-\beta \overline{V_2^{\dagger}}} \right\rangle. \quad (15)$$

The average in Eq. (14) is on the configurations of two ring polymers of  $P$  beads, whereas the average in Eq. (15) is on just one ring polymer of  $2P$  beads (and mass  $m/2$ ). In any case, the configurations are sampled according to the distribution  $F$

described above. The average potentials are defined as

$$\overline{V_2^{\cdot}}(\mathbf{r}) = \frac{1}{P} \sum_{i=1}^P u_2 \left( \left| \mathbf{r} + \mathbf{r}_i^{(1)} - \mathbf{r}_i^{(2)} \right| \right) \quad (16)$$

$$\overline{V_2^{\dagger}} = \frac{1}{P} \sum_{i=1}^P u_2 \left( \left| \mathbf{r}_i^{(3)} - \mathbf{r}_{i+P}^{(3)} \right| \right), \quad (17)$$

where  $\mathbf{r}_i^{(1)}$  and  $\mathbf{r}_i^{(2)}$  in Eq. (16) denote the coordinates of two independent ring polymers of  $P$  beads each, and  $\mathbf{r}_i^{(3)}$  in Eq. (17) denotes the coordinates of a ring polymer of  $2P$  beads. The factor  $\Lambda^3/2^{3/2}$  in Eq. (15) comes from how the action of the permutation operator  $P^{\dagger}$  on the product of the probability distributions  $F$  of two  $P$ -monomer polymers produces the probability distribution of a  $2P$ -monomer coalesced polymer.<sup>9</sup>

## B. The third virial coefficient

The same considerations leading to Eq. (10) can be applied to the three-particle partition function appearing in the expression of  $C(T)$ . In this case, the six permutations of three particles can be conveniently divided into three subsets. The first set includes only the identity permutation, whose representation we will denote as  $P^{\cdot\cdot\cdot}$ . The second set includes the three permutations that swap two particles (which are odd in character), whose representation will be denoted by  $P^{\dagger\dagger\dagger}$ , whereas the third set includes the two remaining cyclic permutations, which are even, and will be denoted by  $P^{\Delta\Delta\Delta}$ . The analogous expression to Eq. (10) is then

$$Q_3(V, T) = \frac{1}{3!} \left( n^3 Q_3^{\cdot\cdot\cdot} \pm 3n^2 Q_3^{\dagger\dagger\dagger} + 2n Q_3^{\Delta\Delta\Delta} \right). \quad (18)$$

Using Eqs. (18) and (10) together with (5), one can write Eq. (3) as

$$C(T) = C_{\text{Boltz}} + \frac{(-1)^{2I}}{2I+1} C_{\text{odd}}(T) + \frac{C_{\text{even}}}{(2I+1)^2} \quad (19)$$

$$C_{\text{Boltz}} = \frac{(Z_2^{\cdot} - V^2)^2}{V^2} - \frac{Z_3^{\cdot\cdot\cdot} - 3VZ_2^{\cdot} + 2V^3}{3V} \quad (20)$$

$$C_{\text{odd}}(T) = -\frac{1}{V} (Z_3^{\dagger\dagger\dagger} - VZ_2^{\dagger}) + \frac{2}{V^2} (Z_2^{\cdot} - V^2) Z_2^{\dagger} \quad (21)$$

$$C_{\text{even}}(T) = \frac{1}{V^2} \left( Z_2^{\dagger\Delta\Delta\Delta} - \frac{2}{3} VZ_3^{\Delta\Delta\Delta} \right), \quad (22)$$

where, denoting as  $\overline{V_3^{\cdot\cdot\cdot}}$  the total three-body energy when two particles are coalesced into a single ring polymer and by  $\overline{V_3^{\Delta\Delta\Delta}}$

the total three-body energy when three particles are coalesced in a single ring polymer,<sup>9</sup> we have

$$\frac{Z_3^{\cdot\cdot}}{V} = \int d\mathbf{r}_1 d\mathbf{r}_2 \left\langle \exp\left(-\beta \overline{V}_3^{\cdot\cdot}(\mathbf{r}_1, \mathbf{r}_2)\right) \right\rangle \quad (23)$$

$$\frac{Z_3^{\cdot\mid}}{V} = \frac{\Lambda^3}{2^{3/2}} \int d\mathbf{r} \left\langle \exp\left(-\beta \overline{V}_3^{\cdot\mid}(\mathbf{r})\right) \right\rangle \quad (24)$$

$$\frac{Z_3^{\Delta}}{V} = \frac{\Lambda^6}{3^{3/2}} \left\langle \exp\left(-\beta \overline{V}_3^{\Delta}\right) \right\rangle, \quad (25)$$

where, analogously to Eqs. (16) and (17), we have defined

$$\overline{V}_3^{\cdot\cdot}(\mathbf{r}_1, \mathbf{r}_2) = \frac{1}{P} \sum_{i=1}^P V_3(\mathbf{r}_1 + \mathbf{r}_i^{(1)}, \mathbf{r}_2 + \mathbf{r}_i^{(2)}, \mathbf{r}_{i+P}^{(3)}) \quad (26)$$

$$\overline{V}_3^{\cdot\mid}(\mathbf{r}) = \frac{1}{P} \sum_{i=1}^P V_3(\mathbf{r}_i^{(1)}, \mathbf{r} + \mathbf{r}_i^{(4)}, \mathbf{r} + \mathbf{r}_{i+P}^{(4)}) \quad (27)$$

$$\overline{V}_3^{\Delta} = \frac{1}{P} \sum_{i=1}^P V_3(\mathbf{r}_i^{(5)}, \mathbf{r}_{i+P}^{(5)}, \mathbf{r}_{i+2P}^{(5)}). \quad (28)$$

In Eqs. (26)–(28),  $\mathbf{r}_i^{(k)}$  for  $k = 1, 2, 3$  are the coordinates of independent  $P$ -bead ring polymers,  $\mathbf{r}_i^{(4)}$  are the coordinates of a ring polymer with  $2P$  beads and mass  $m/2$ , and  $\mathbf{r}_i^{(5)}$  denote the coordinates of a ring polymer with  $3P$  beads and mass  $m/3$ . Note that we have slightly changed the notation from Refs. 9 and 10, by collecting together all the terms with an odd or even character upon particle exchange.

### C. The fourth virial coefficient

The permutation group of 4 particles has an even richer structure. For our purposes, it is sufficient to recall the pres-

ence of the following subsets:

- The identity element, whose representation we will denote as  $P^{\cdot\cdot\cdot}$ . In this case the sum over the internal states gives a factor  $n^4$ .
- The swapping of a single pair. This subset has odd parity, and includes 6 elements. Its representation will be denoted by  $P^{\cdot\mid\mid}$ . The sum over the internal states results in a factor  $n^3$ .
- The cyclic permutation on subsets of 3 particles. This subset has an even parity and includes 8 elements. Its representation will be denoted by  $P^{\Delta\Delta}$ . The sum on the internal states produces a factor of  $n^2$ .
- The swapping of two distinct pairs. This subset has even parity and includes 3 elements. Its representation will be denoted by  $P^{\parallel\parallel}$ . Also in this case the sum over the internal states produces a factor  $n^2$ .
- The 6 remaining permutations all produce a single ring polymer. This subset has odd parity and includes, for example, the cyclic permutations. Its representation will be denoted by  $P^{\square}$ , and the sum over the internal states produces a factor of  $n$ .

We can then write the 4-particle partition function as

$$Q_4(V, T) = \frac{1}{4!} \left( n^4 Q_4^{\cdot\cdot\cdot} \pm 6n^3 Q_4^{\cdot\mid\mid} + 8n^2 Q_4^{\Delta\Delta} + 3n^2 Q_4^{\parallel\parallel} \pm 6n Q_4^{\square} \right), \quad (29)$$

and the expression for  $D(T)$  turns out to be, after lengthy but straightforward calculations,

$$D(T) = D_{\text{Boltz}}(T) + D_{\text{xc}}(T) \quad (30)$$

$$D_{\text{Boltz}}(T) = -\frac{Z_4^{\cdot\cdot} - 4VZ_3^{\cdot\cdot} - 3(Z_2^{\cdot\cdot})^2 + 12V^2Z_2^{\cdot\cdot} - 6V^4}{8V} + \frac{3(Z_2^{\cdot\cdot} - V^2)(Z_3^{\cdot\cdot} - 3VZ_2^{\cdot\cdot} + 2V^3)}{2V^2} - \frac{5(Z_2^{\cdot\cdot} - V^2)^3}{2V^3} \quad (31)$$

$$D_{\text{xc}}(T) = \frac{(-1)^{2I}}{2I+1} D_{01}(T) + \frac{1}{(2I+1)^2} D_{e1}(T) + \frac{(-1)^{2I}}{(2I+1)^3} D_{02}(T) \quad (32)$$

$$= D_{01}(T) + D_{e1}(T) + D_{02}(T) \quad [\text{for } {}^4\text{He}] \quad (33)$$

$$= \frac{-1}{2} D_{01}(T) + \frac{1}{4} D_{e1}(T) + \frac{-1}{8} D_{02}(T) \quad [\text{for } {}^3\text{He}] \quad (34)$$

$$D_{01}(T) = -\frac{3}{4V} \left( Z_4^{\cdot\mid} - 2VZ_3^{\cdot\mid} - Z_2^{\cdot\mid}Z_2^{\cdot\mid} + 2V^2Z_2^{\cdot\mid} \right) + \frac{9}{2V^2} (Z_2^{\cdot\cdot} - V^2)(Z_3^{\cdot\mid} - VZ_2^{\cdot\mid}) + \frac{3}{2V^2} \left( Z_3^{\cdot\mid} - 3VZ_2^{\cdot\mid} + 2V^3 \right) Z_2^{\cdot\mid} - \frac{15}{2V^3} (Z_2^{\cdot\cdot} - V^2)^2 Z_2^{\cdot\mid} \quad (35)$$

$$D_{e1}(T) = -\frac{(Z_4^{\Delta\Delta} - VZ_3^{\Delta\Delta})}{V} - \frac{3(Z_4^{\parallel\parallel} - Z_2^{\parallel\parallel})}{8V} + \frac{3(Z_2^{\cdot\cdot} - V^2)Z_3^{\Delta\Delta}}{V^2} + \frac{9Z_2^{\mid}(Z_3^{\cdot\mid} - VZ_2^{\cdot\mid})}{2V^2} - \frac{15(Z_2^{\cdot\cdot} - V^2)Z_2^{\mid\mid}}{2V^3} \quad (36)$$

$$D_{02}(T) = -\frac{3}{4V} Z_4^{\square} + \frac{3}{V^2} Z_2^{\mid}Z_3^{\Delta\Delta} - \frac{5}{2V^3} Z_2^{\mid\mid\mid}, \quad (37)$$

where, denoting again with  $\overline{V}_4^{\sigma}$  the total four-body potential

energy for the equivalent classical system obtained by apply-

ing the permutation  $\sigma$ , we have defined

$$\frac{Z_4^{\ddot{\cdot}}}{V} = \int d\mathbf{r}_1 d\mathbf{r}_2 d\mathbf{r}_3 \langle \exp(-\beta \overline{V}_4^{\ddot{\cdot}}) \rangle \quad (38)$$

$$\frac{Z_4^{\dot{\cdot}}}{V} = \frac{\Lambda^3}{2^{3/2}} \int d\mathbf{r}_1 d\mathbf{r}_2 \left\langle \exp\left(-\beta \overline{V}_4^{\dot{\cdot}}\right) \right\rangle \quad (39)$$

$$\frac{Z_4^{\parallel}}{V} = \frac{\Lambda^6}{8} \int d\mathbf{r} \left\langle \exp\left(-\beta \overline{V}_4^{\parallel}\right) \right\rangle \quad (40)$$

$$\frac{Z_4^{\Delta}}{V} = \frac{\Lambda^6}{3^{3/2}} \int d\mathbf{r} \left\langle \exp\left(-\beta \overline{V}_4^{\Delta}\right) \right\rangle \quad (41)$$

$$\frac{Z_4^{\square}}{V} = \frac{\Lambda^9}{8} \left\langle \exp\left(-\beta \overline{V}_4^{\square}\right) \right\rangle, \quad (42)$$

with

$$\overline{V}_4^{\ddot{\cdot}}(\mathbf{r}_1, \mathbf{r}_2, \mathbf{r}_3) = \frac{1}{P} \sum_{i=1}^P V_4 \left( \mathbf{r}_1 + \mathbf{r}_i^{(1)}, \mathbf{r}_2 + \mathbf{r}_i^{(2)}, \mathbf{r}_3 + \mathbf{r}_i^{(3)}, \mathbf{r}_i^{(4)} \right) \quad (43)$$

$$\overline{V}_4^{\dot{\cdot}}(\mathbf{r}_1, \mathbf{r}_2) = \frac{1}{P} \sum_{i=1}^P V_4 \left( \mathbf{r}_1 + \mathbf{r}_i^{(1)}, \mathbf{r}_2 + \mathbf{r}_i^{(2)}, \mathbf{r}_i^{(5)}, \mathbf{r}_{i+P}^{(5)} \right) \quad (44)$$

$$\overline{V}_4^{\parallel}(\mathbf{r}) = \frac{1}{P} \sum_{i=1}^P V_4 \left( \mathbf{r}_i^{(5)}, \mathbf{r}_{i+P}^{(5)}, \mathbf{r} + \mathbf{r}_i^{(6)}, \mathbf{r} + \mathbf{r}_{i+P}^{(6)} \right) \quad (45)$$

$$\overline{V}_4^{\Delta}(\mathbf{r}) = \frac{1}{P} \sum_{i=1}^P V_4 \left( \mathbf{r} + \mathbf{r}_i^{(1)}, \mathbf{r}_i^{(7)}, \mathbf{r}_{i+P}^{(7)}, \mathbf{r}_{i+2P}^{(7)} \right) \quad (46)$$

$$\overline{V}_4^{\square} = \frac{1}{P} \sum_{i=1}^P V_4 \left( \mathbf{r}_i^{(8)}, \mathbf{r}_{i+P}^{(8)}, \mathbf{r}_{i+2P}^{(8)}, \mathbf{r}_{i+3P}^{(8)} \right). \quad (47)$$

In Eqs. (43)–(47),  $\mathbf{r}_i^{(k)}$  with  $k = 1, 2, 3, 4$  are the coordinates of independent  $P$ -bead ring polymers,  $\mathbf{r}_i^{(k)}$  with  $k = 5, 6$  are the coordinates of independent  $2P$ -bead ring polymers and mass  $m/2$ ,  $\mathbf{r}_i^{(7)}$  are the coordinates of a  $3P$ -bead ring polymer and mass  $m/3$ , and  $\mathbf{r}_i^{(8)}$  are the coordinates of a  $4P$ -bead ring polymer and mass  $m/4$ .

### III. NUMERICAL CALCULATIONS

In order to find the optimal number of monomers  $P$  as a function of temperature in the ring-polymer representation of the quantum problem, we reanalyzed highly accurate calculations of  $B(T)$  to find the values  $P(T)$  above which the calculated  $B$  did not change within about one part in  $10^4$ . We found that convergence in the investigated range of temperature was assured by choosing  $P$  equal to  $\text{nint}(4 + 620/(T/1 \text{ K})^{0.7})$  in the case of  ${}^4\text{He}$  and  $\text{nint}(4 + 770/(T/1 \text{ K})^{0.7})$  in the case of  ${}^3\text{He}$ , where  $\text{nint}(x)$  denotes the nearest integer to  $x$ . With this choice, the values of  $P$  are close to what we have used in our previous work for  $T > 10 \text{ K}$ , but optimize the utilization of numerical resources in the low-temperature regime where degeneracy is important.

In our calculations of  $D(T)$ , we performed the multidimensional integrations in Eqs. (30)–(42) using the parallel implementation of the VEGAS algorithm.<sup>21,22</sup> The six-dimensional integrations leading to  $D_{\text{Boltz}}$  were performed using  $4 \times 10^6$

Monte Carlo calls, the three-dimensional integrations leading to  $D_{01}$  using  $5 \times 10^5$  calls, and the one-dimensional integrations leading to  $D_{e1}$  using 5000 calls. The averages appearing in Eqs. (38)–(42) were evaluated using independent ring polymers generated by the prescription of Levy.<sup>23,24</sup> The number of ring polymers depends on the specific contribution to  $D(T)$ : we used 16 in the case of  $D_{\text{Boltzmann}}$ , 128 for  $D_{01}$  and  $D_{e1}$ , and  $3 \times 10^6$  for the evaluation of  $D_{02}$ . Following Kofke and coworkers,<sup>14,15</sup> we found it convenient to evaluate separately the two-body contribution to the various components of  $D(T)$  and the difference leading to the full calculation involving the three-body potential.

We used the very recent two-body potential by Czachorowski *et al.*<sup>7</sup> and the three-body potential by Cencek *et al.*<sup>13</sup> To the best of our knowledge, no four-body potential is available for helium, so in this work we set it to zero. The additional uncertainty due to this assumption is discussed in Sec. IV C.

The evaluation of  $D(T)$  using the procedure outlined above is quite CPU-intensive. At the lowest temperature investigated here, where the calculations are more demanding, we needed roughly 20 000 CPU-hours on a modern 2.5 GHz processor, half of which are dedicated to the evaluation of the exchange contributions. The requirements are roughly inversely proportional to the temperature, hence we needed 4000 CPU-hours at  $T = 10 \text{ K}$ , 650 CPU-hours at 120 K, and so on.

## IV. ESTIMATION OF UNCERTAINTIES

### A. PIMC statistical uncertainty

The statistical uncertainty of the PIMC calculations was evaluated as the standard error of the mean of a set of independent calculations. The number of independent calculations that we employed varied according to the component of  $D(T)$  that was calculated. We used 8 for the Boltzmann component, 24 for  $D_{01}$ , 64 for  $D_{e1}$  and  $D_{02}$ . The VEGAS algorithm produces its own estimation of standard uncertainty, which we verified was in very good agreement with the estimate based on independent calculations.

### B. Uncertainty propagated from potentials

The usual way to evaluate the contribution to the overall uncertainty of virial coefficients due to the potentials is to perform the calculation with perturbed two- and three-body potentials (where the size of the perturbation is the estimated uncertainty of the potential) and take the difference. Given the considerable computing requirements for the evaluation of  $D(T)$ , we examined a more efficient way to propagate the uncertainty from the potentials to the fourth virial coefficient, starting from the functional derivative of Eq. (4) with respect to the  $k$ -body irreducible potentials  $u_k(\mathbf{r}_1, \dots, \mathbf{r}_k)$  that  $D(T)$  depends on. We begin by noticing that in the classical limit,

the functions  $Z_N$  become

$$Z_N = \int e^{-\beta V_N(\mathbf{r}_1, \dots, \mathbf{r}_N)} \prod_{i=1}^N d^3 \mathbf{r}_i, \quad (48)$$

and that the variation of the  $n$ -th virial coefficient,  $B_n$ , can be written as

$$\delta B_n^{(k)} = \int \frac{\delta B_n}{\delta u_k(\mathbf{r}_1, \dots, \mathbf{r}_k)} \delta u_k(\mathbf{r}_1, \dots, \mathbf{r}_k) \prod_{i=1}^k d^3 \mathbf{r}_i, \quad (49)$$

where  $\delta B_n / \delta u_k$  is the functional derivative of the virial coefficient with respect to the  $k$ -body irreducible potential. From Eq. (48) one has

$$\frac{\delta Z_2}{\delta u_2(\mathbf{r}_1, \mathbf{r}_2)} = -\beta \exp[-\beta u_2(\mathbf{r}_1, \mathbf{r}_2)] \quad (50)$$

$$\frac{\delta Z_3}{\delta u_2(\mathbf{r}_1, \mathbf{r}_2)} = -3\beta \int \exp[-\beta V_3(\mathbf{r}_1, \mathbf{r}_2, \mathbf{r}_3)] d\mathbf{r}_3 \quad (51)$$

$$\frac{\delta Z_3}{\delta u_3(\mathbf{r}_1, \mathbf{r}_2, \mathbf{r}_3)} = -\beta \exp[-\beta V_3(\mathbf{r}_1, \mathbf{r}_2, \mathbf{r}_3)] \quad (52)$$

$$\frac{\delta Z_4}{\delta u_2(\mathbf{r}_1, \mathbf{r}_2)} = -6\beta \int \exp[-\beta V_4(\mathbf{r}_1, \dots, \mathbf{r}_4)] d\mathbf{r}_3 d\mathbf{r}_4 \quad (53)$$

$$\frac{\delta Z_4}{\delta u_3(\mathbf{r}_1, \mathbf{r}_2, \mathbf{r}_3)} = -4\beta \int \exp[-\beta V_4(\mathbf{r}_1, \dots, \mathbf{r}_4)] d\mathbf{r}_4 \quad (54)$$

$$\frac{\delta Z_4}{\delta u_4(\mathbf{r}_1, \mathbf{r}_2, \mathbf{r}_3, \mathbf{r}_4)} = -\beta \exp[-\beta V_4(\mathbf{r}_1, \dots, \mathbf{r}_4)], \quad (55)$$

enabling evaluation of  $\delta D$  by functional differentiation of Eq. (4). Actually, one can evaluate the variation of  $D(T)$  with respect to the two- and three-body potentials separately; using as an example the variation due to a perturbation of the pair potential, an expression is obtained of the form

$$\delta D^{(2)}(T) = \int \delta u_2(\mathbf{r}_1, \mathbf{r}_2) \frac{\delta D}{\delta u_2(\mathbf{r}_1, \mathbf{r}_2)} d\mathbf{r}_1 d\mathbf{r}_2. \quad (56)$$

A naive evaluation of the uncertainty using (the absolute value of) Eq. (56) when only  $\delta u_2$  is assumed to be at any point the absolute value of the estimated uncertainty due to the pair potential is at best a lower bound on the actual uncertainty on  $D(T)$ . Actually, the other factor in the integrand, that is the functional derivative  $\delta D / \delta u_2$ , is a function that has negative and positive regions whose relative importance changes with temperature. Our calculations show that the estimated uncertainty using Eq. (56) would cross zero somewhere around  $T = 30$  K. Conversely, a more conservative estimate (possibly resulting in an upper bound) to the propagated uncertainty from the potential to the fourth virial coefficient can be obtained by using the absolute value of the integrand in Eq. (56); we also decided to consider the highest absolute value of  $\delta D / \delta u_2$  when calculated with the most positive ( $u_2^+ = u_2 + \delta u_2$ ) or the most negative ( $u_2^- = u_2 - \delta u_2$ ) pair potential, so that our final expression of the propagated uncertainty due to the  $k$ -body potential is

$$\delta D^{(k)}(T) = \int \left| \delta u_k \frac{\delta D}{\delta u_k} \right| \prod_{i=1}^k d^3 \mathbf{r}_i. \quad (57)$$

We considered the uncertainties associated to the potentials as expanded uncertainties with coverage factor  $k = 2$ , so we obtained the standard uncertainties by dividing by 2 the values obtained using Eq. (57). The standard uncertainties from the pair and three-body potentials were then added in quadrature to obtain the standard uncertainty due to the imperfect knowledge of the potential-energy surfaces.

The final formulae that we obtain are:

$$\begin{aligned} \delta D^{(2)}(T) = & \frac{\beta}{8V} \int \delta u_2(1, 2) \left| 6e^{-\beta V_4(1, 2, 3, 4)} - 12e^{-\beta V_3(1, 2, 3)} - 6e^{-\beta(V_2(1, 2) + V_2(3, 4))} + 12e^{-\beta V_2(1, 2)} \right. \\ & \left. - 12e^{-\beta V_2(1, 2)} \left( e^{-\beta V_3(2, 3, 4)} - 3e^{-\beta V_2(3, 4)} + 2 \right) - 36 \left( e^{-\beta V_3(1, 2, 3)} - e^{-\beta V_2(1, 2)} \right) \left[ e^{-\beta V_2(3, 4)} - 1 \right] \right. \\ & \left. + 60e^{-\beta V_2(1, 2)} \left( e^{-\beta V_2(3, 4)} - 1 \right)^2 \right| \prod_{i=1}^4 d^3 \mathbf{r}_i, \end{aligned} \quad (58)$$

$$\delta D^{(3)}(T) = \frac{\beta}{8V} \int \delta u_3(1, 2, 3) \left| 4e^{-\beta V_4(1, 2, 3, 4)} - 4e^{-\beta V_3(1, 2, 3)} + 12e^{-\beta V_3(1, 2, 3)} \left( e^{-\beta V_2(3, 4)} - 1 \right) \right| \prod_{i=1}^4 d^3 \mathbf{r}_i, \quad (59)$$

where in actual numerical integration it can be useful to consider that the final result must be invariant under any permutation of the four particles' coordinates so that, for exam-

ple, one can use  $4e^{-\beta V_3(1, 2, 3)} = e^{-\beta V_3(1, 2, 3)} + e^{-\beta V_3(2, 3, 4)} + e^{-\beta V_3(3, 4, 1)} + e^{-\beta V_3(4, 1, 2)}$ . Our final estimate for the propa-

gated uncertainty due to the potential is then

$$u_V(D) = \frac{1}{4} \sqrt{(\delta D^{(2)}(T))^2 + (\delta D^{(3)}(T))^2}. \quad (60)$$

In order to take into account the quantum nature of helium, we used the unchanged three-body potential together with the fourth-order Feynman–Hibbs semiclassical pair potential<sup>25</sup> to evaluate Eq. (57).

$$u_{\text{FH4}}(r) = u_2(r) + \frac{\beta \hbar^2}{12m} \left( u_2''(r) + \frac{2u_2'(r)}{r} \right) + \frac{1}{2} \left( \frac{\beta \hbar^2}{12m} \right)^2 \left( u_2'''(r) + \frac{4u_2''(r)}{r} \right). \quad (61)$$

In Eq. (61), the number of primes indicates the order of the derivative which, in our calculations, have been evaluated numerically using the central-difference formulae with a grid spacing  $\delta r = 10^{-3}$  Å. We found that this approach provided very good estimates for the uncertainty of  $B(T)$  and  $C(T)$ , when compared with the traditional way of calculating this contribution,<sup>5,11,26,27</sup> down to roughly  $T = 4$  K, corresponding to the onset of quantum exchange effects, which are not taken into account in this procedure. Below this threshold, the semiclassical estimation is likely to produce an upper bound on the actual uncertainty, since using the quadratic Feynman–Hibbs potential in Eqs. (58) and (59) produces a larger estimate of the uncertainty than the quartic used here.

At the lowest temperatures, we checked whether the approximations used to evaluate  $u_V(D)$  were still good by running calculations with perturbed potentials and taking one fourth of the difference of the values of  $D(T)$  obtained in this way, as in our previous work. Since the statistical uncertainty is large in this regime, we took the conservative approach of adding one fourth of the combined uncertainties of  $D(T)$  with the perturbed potentials to generate an estimate of  $u_V(D)$ . We found this estimate to be compatible with the one obtained using the procedure described in this section in the case of  ${}^4\text{He}$ . In the case of  ${}^3\text{He}$ , the semiclassical estimation of  $u_V(D)$  produces a value of  $2 \times 10^5$  cm<sup>9</sup> mol<sup>-3</sup> at  $T = 2.6$  K which is four times as large as the value of  $D(T)$ , hence the approach described in this section is definitely questionable at the lowest temperatures. Analogously to the case of  ${}^4\text{He}$ , we performed calculations with the perturbed potentials, finding a good agreement above  $T = 5$  K. For lower temperatures, we report as  $u_V(D)$  the values obtained using the difference of the PIMC simulation with perturbed potentials combined with the statistical uncertainty.

### C. Uncertainty due to four-body potential

We performed these calculations with high-accuracy pair<sup>7</sup> and three-body<sup>13</sup> potentials. While this truncation of the many-body expansion is rigorous for the third virial coefficient, the fourth virial coefficient is affected by any four-body nonadditivity that might exist. Unfortunately, there have been few attempts to calculate four-body interactions for helium,

and to our knowledge no four-body potential has been developed. Our analysis of this uncertainty contribution must therefore involve some guesswork and approximations.

Because helium is not very polarizable, the multibody forces are weak and the multibody expansion should converge quickly. This is reflected in the behavior of  $C(T)$ , where almost all of the quantity is given by the pair potential and the contribution of the three-body potential is on the order of 1% to 2%.<sup>26</sup> We find similar behavior for  $D(T)$ , where the three-body effect is much smaller than the two-body contribution at most temperatures. At high temperatures, however, the relative contribution of three-body effects becomes large (on the order of 30% at 2000 K); this is probably an artifact of the absolute value of  $D$  becoming small. Because of the apparent rapid convergence of the multibody expansion, a rough estimate for the effect of four-body forces might be 10% of the size of the three-body effect.

In order to be more quantitative, we considered the four-body potential developed by Bade in the framework of the Drude model of dispersion.<sup>28,29</sup> This model takes into account only long-range dispersion, so that it results in a pair potential with a  $r^{-6}$  dependence and in the case of three-body forces it reproduces the Axilrod–Teller form. It has been used to estimate the contribution of four-body forces to  $D(T)$  in the cases of neon and argon.<sup>30,31</sup> Bade’s potential depends on the single-atom polarizability  $\alpha_1$ , which is known both experimentally and theoretically with high precision for He,<sup>32,33</sup> and an unknown parameter – named  $\hbar\omega_0$  or  $V$  in the original papers – that we fixed from the knowledge of the coefficient of  $r^{-6}$  term in the most recent pair potential for He.<sup>7</sup> With this choice, Bade’s model produces a value for the Axilrod–Teller parameter for He that is within 4% of the actual value.<sup>34</sup> We then proceeded to evaluate the contribution to  $D(T)$  from this four-body potential, using a semiclassical approach with the 4th-order Feynmann–Hibbs expression for the pair potential. As might be expected based on the convergence of the many-body expansion, this contribution is on the order of 10% of the three-body contribution, except near 5 K where the three-body contribution crosses zero.

However, Bade’s model is purely for dispersion interactions; it does not take into account the repulsive part of the four-body potential. For  $C(T)$ , it is known that the Axilrod–Teller three-body dispersion effect is only accurate at low temperatures; the repulsive nonadditivity has the opposite sign and becomes a larger contribution to  $C(T)$  above approximately 170 K.<sup>26</sup> The magnitude of this repulsive contribution is similar to the size of the Axilrod–Teller contribution, so similar behavior might be expected for the contribution of repulsive nonadditivity to  $D(T)$ . We therefore estimated an uncertainty contribution due to the missing four-body potential as the maximum of 15% of the absolute value of the three-body contribution (interpolated at those temperatures where we did not calculate it) and the absolute value of the dispersion contribution estimated from Bade’s potential. We consider this an expanded uncertainty with coverage factor  $k = 2$ . The corresponding standard uncertainty is reported in Table I for  ${}^4\text{He}$  and in Table III for  ${}^3\text{He}$  in the column labeled  $u_4(D)$ .

## V. RESULTS AND DISCUSSION

### A. Calculated $D(T)$

We report the results of our calculations for  ${}^4\text{He}$  in Tables I and II, where we also compare our results with the values reported by the group of Kofke.<sup>14,15</sup> In general, we obtain very good agreement for the Boltzmann contribution to  $D(T)$ , although the statistical uncertainties of our calculations are generally larger. In order to produce Boltzmann values of lower uncertainty based on all data, we combined their results with ours at the temperatures where both studies reported results, with statistical weighting according to the uncertainty from each source:

$$D = \frac{\frac{D_{\text{TW}}}{u(D_{\text{TW}})^2} + \frac{D_{\text{KG}}}{u(D_{\text{KG}})^2}}{u(D_{\text{TW}})^{-2} + u(D_{\text{KG}})^{-2}} \quad (62)$$

$$u(D) = \sqrt{\frac{1}{u(D_{\text{TW}})^{-2} + u(D_{\text{KG}})^{-2}}}, \quad (63)$$

where the subscript TW indicates the values calculated in this work, and the subscript KG indicates the value from Kofke's group.

At temperatures above about 8 K, the uncertainty budget is dominated by the uncertainty due to the imperfect knowledge of the potentials. At the lower end of this temperature range, inspection of the contributions to  $u_V(D)$  shows that this is mainly due to the uncertainty of the three-body potential. Above about 20 K, the uncertainty is dominated by  $u_4(D)$ , the uncertainty due to possible four-body interactions. At the lowest temperatures, the statistical uncertainty from the PIMC calculations (primarily the calculation of  $D_{\text{Boltz}}$ ) becomes a sizable contribution to the overall uncertainty budget.

The effect of the exchange terms on  $D(T)$  is minimal, at least in the case of  ${}^4\text{He}$ . Inspection of Table I shows that the values of  $D_{\text{xc}}(T)$  have an uncertainty comparable to their absolute value. The breakdown of all the contributions, reported in Table II, shows that  $D_{\text{xc}}(T)$  is obtained as the sum of terms with opposite signs and comparable magnitude, resulting in consistent cancellations.

The situation for  ${}^3\text{He}$ , reported in Tables III and IV, is qualitatively similar to that of the heavier isotope, with two notable differences. First, the fourth virial coefficient increases with decreasing temperature in the whole range considered, different from the case of  ${}^4\text{He}$  where a maximum is observed around  $T = 4.5$  K. Second, the fermionic nature of  ${}^3\text{He}$  is such that the various contributions to  $D_{\text{xc}}(T)$  in Eq. (34) are all positive, resulting in a net positive value of the exchange terms in the whole range considered. Because the group of Kofke did not report calculations for  ${}^3\text{He}$ ,<sup>14,15</sup> the values of  $D_{\text{Boltz}}(T)$  in Table III are only those resulting from our calculations.

### B. Comparison with experimental data

While the virial coefficients in Eq. (1) can be extracted from experimental measurements, in practice this becomes quite

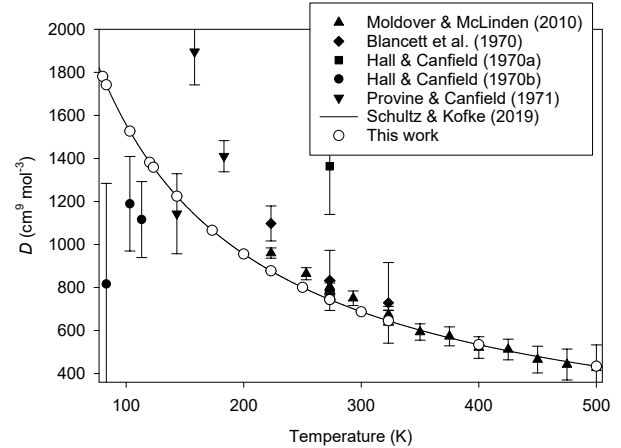


FIG. 1. Comparison of calculated values of  $D(T)$  for  ${}^4\text{He}$  with experimental results<sup>35–38,40</sup> and with correlation fitted to first-principles calculations by Schultz and Kofke.<sup>15</sup> Error bars represent expanded uncertainties with coverage factor  $k = 2$ . Expanded uncertainties for this work are smaller than the size of the symbols; see Table I.

difficult for the higher coefficients because they require extracting higher-order effects (a third derivative in the case of  $D$ ). Relatively high pressures are also necessary to reach densities where  $D(T)$  is significant.

The Burnett method of systematic expansions between two vessels of similar size can reduce the uncertainties in measuring virial coefficients. This method was used by Canfield and coworkers in a series of papers on helium and its mixtures with other gases, several of which reported virial coefficients up to the fourth for helium at various temperatures.<sup>35–38</sup> None of these papers reported a full uncertainty analysis; when plotting these points we use the parameter uncertainties reported in the papers, which appear to be only the statistical uncertainties from their fits to their data.

Highly accurate measurements on helium were performed by McLinden and Lösch-Will<sup>39</sup> with a two-sinker magnetic-suspension densimeter. The same method was used by Moldover and McLinden,<sup>40</sup> who reanalyzed both their data and the earlier measurements.<sup>39</sup> This analysis was constrained with *ab initio* values of  $B(T)$ <sup>5</sup> and  $C(T)$ ,<sup>26</sup> allowing them to reduce the uncertainty of  $D$  on each isotherm by a factor of 6 compared to unconstrained analysis.

In Fig. 1, our results from Table I are shown along with the experimental data for  ${}^4\text{He}$ . The data from the Burnett experiments of 50 years ago<sup>35–38</sup> are in qualitative agreement with our results, but are too scattered for meaningful quantitative comparison. The results of Moldover and McLinden<sup>40</sup> are in excellent agreement with our calculations above 300 K. At lower temperatures, there is a disagreement which is small but outside the mutual uncertainties. We note that the points of Moldover and McLinden that agree well are all from their “2007 isotherms,” while their points from “2005 isotherms” show a systematic offset. This may suggest an unrecognized problem with the 2005 experiments. The 2007 isotherms were measured with new sinkers whose volumes were newly cali-

TABLE I. The fourth virial coefficient of  $^4\text{He}$  and its contributions:  $D_{\text{Boltz,TW}}(T)$ , Boltzmann contribution calculated in this work;  $D_{\text{Boltz,KG}}(T)$ , Boltzmann contribution from Ref. 14;  $D_{\text{Boltz}}(T)$ , combined Boltzmann values from this work and Ref. 14;  $D_{\text{xc}}(T)$  exchange contribution;  $u_V(D)$ , propagated uncertainty from the pair and three-body potential;  $u_4(D)$ , estimated uncertainty due to the neglect of the four-body potential;  $D(T)$ , final values. The numbers in parentheses report standard uncertainty on the last digits. In the last column, the combined expanded uncertainty of  $D(T)$  is reported at  $k = 2$  coverage.

Temperature (K)	$D_{\text{Boltz,TW}}(T)$ (cm $^9$ mol $^{-3}$ )	$D_{\text{Boltz,KG}}(T)$ (cm $^9$ mol $^{-3}$ )	$D_{\text{Boltz}}(T)$ (cm $^9$ mol $^{-3}$ )	$D_{\text{xc}}(T)$ (cm $^9$ mol $^{-3}$ )	$u_V(D)$ (cm $^9$ mol $^{-3}$ )	$u_4(D)$ (cm $^9$ mol $^{-3}$ )	$D(T)$ (cm $^9$ mol $^{-3}$ )	$U(D)$ (cm $^9$ mol $^{-3}$ )
2.6	-242000(12000)	-238000(8000)	-239000(7000)	-900(3000)	15000	1400	-240000	30000
2.8		-120000(6000)	-120000(6000)	-1100(2300)	8000	900	-120000	20000
3	-53000(6000)	-61000(4000)	-58000(3000)	700(1000)	4000	600	-60000	11000
3.25		-17000(3000)	-17000(3000)	1100(600)	3000	300	-16000	8000
3.5		6000(2000)	6000(2000)	-200(400)	1700	300	6000	5000
3.75		12400(1500)	12000(1500)	0(300)	1100	200	12000	4000
4	19000(2000)	19500(1100)	19400(1000)	160(80)	800	180	20000	3000
4.25		20800(900)	20800(900)	50(120)	600	160	21000	2000
4.5		22500(700)	22500(700)	54(80)	500	140	23000	1700
4.75		21000(500)	21000(500)	-49(40)	400	120	21000	1300
5	21100(900)	19200(400)	19500(400)	-17(20)	300	110	19500	1000
5.25		17300(400)	17300(400)	-1(20)	300	100	17300	1000
5.5		16100(300)	16100(300)	-22(12)	200	100	16100	800
6	13800(500)	13200(200)	13300(190)	-4(4)	170	90	13300	500
7	8800(300)	9100(130)	9000(120)	-1.3(13)	110	70	9000	300
8	6200(200)		6200(200)		70	60	6200	500
8.5		5730(60)	5730(60)		60	50	5700	200
10	4100(100)	4100(30)	4100(30)		40	40	4100	140
15	2880(40)		2880(40)		17	30	2900	110
20	2768(16)	2782(3)	2781(3)		9	20	2780	50
24.5561		2740.1(14)	2740.1(14)		6	18	2740	40
30	2665(6)	2659.0(8)	2659.1(8)		4	15	2660	30
40		2462.5(3)	2462.5(3)		3	11	2460	20
50	2256.7(18)	2259.90(19)	2259.90(19)		2	9	2260	19
63.15		2025.61(12)	2025.61(12)		1.4	8	2030	15
80	1781.3(7)		1781.3(7)		1.1	6	1781	13
83.15		1742.22(7)	1742.22(7)		1.1	6	1742	12
103.15		1526.67(4)	1526.67(4)		0.9	5	1527	10
120	1381.7(5)		1381.7(5)		0.8	4	1382	9
123.15		1358.59(4)	1358.59(4)		0.8	4	1359	9
143.15		1224.22(3)	1224.22(3)		0.7	4	1224	8
173.15		1066.096(16)	1066.096(16)		0.6	3	1066	6
200	955.4(4)		955.4(4)		0.6	3	955	6
223.15		876.991(16)	876.991(16)		0.6	3	877	5
250	800.1(3)		800.1(3)		0.5	2	800	5
273.15		744.051(12)	744.051(12)		0.5	2	744	5
273.16	743.5(3)		743.5(3)		0.5	2	744	5
300	687.0(3)		687.0(3)		0.5	2	687	4
323.15		645.170(10)	645.170(10)		0.5	2	645	4
400	534.0(2)	534.115(7)	534.115(7)		0.5	2	534	4
500	433.9(2)	434.029(5)	434.029(5)		0.4	2	434	4
600		363.438(5)	363.438(5)		0.4	2	363	4
700	310.80(18)	310.920(4)	310.920(4)		0.4	2	311	4
800		270.314(4)	270.314(4)		0.4	1.9	270	4
900		238.021(4)	238.021(4)		0.4	1.9	238	4
1000	211.50(14)	211.702(3)	211.702(3)		0.4	1.9	212	4
1500	130.43(10)		130.43(10)		0.3	1.7	130	4
2000	89.14(8)		89.14(8)		0.3	1.6	89	3

brated; it is plausible that there may have been a small error in calibration for the sinkers used in 2005.<sup>41</sup> Figure 1 also shows the equation that Schultz and Kofke<sup>15</sup> fit to their results at 20 K and above, which were calculated using Boltzmann

statistics only. It is not surprising that this equation is in excellent agreement with our results, since exchange effects are negligible at these temperatures.

TABLE II. The exchange contributions to  $D(T)$  for  $^4\text{He}$ , see Eqs. (30)–(37). Uncertainties here are  $k = 1$ .

Temperature (K)	$D_{01}(T)$ (cm $^9$ mol $^{-3}$ )	$D_{e1}(T)$ (cm $^9$ mol $^{-3}$ )	$D_{02}(T)$ (cm $^9$ mol $^{-3}$ )	$D_{xc}(T)$ (cm $^9$ mol $^{-3}$ )
2.6	-5716(2663)	11324(1297)	-6475(73)	-867(2963)
2.8	-3163(2236)	5072(544)	-2989(23)	-1081(2301)
3	-2960(887)	5118(449)	-1464(17)	695(995)
3.25	-286(585)	1945(149)	-596(5)	1062(603)
3.5	-839(438)	856(84)	-258(3)	-241(446)
3.75	-491(298)	580(54)	-113.9(13)	-25(303)
4	-198(74)	407(33)	-51.9(9)	158(81)
4.25	-77(116)	151(14)	-24.6(4)	50(117)
4.5	-46(75)	111(10)	-11.6(2)	54(75)
4.75	-91(40)	47(6)	-5.64(11)	-49(40)
5	-47(21)	32(3)	-1.39(4)	-17(21)
5.25	-21(22)	21(2)	-0.73(2)	-1(22)
5.5	-27(12)	7.9(15)	-2.85(7)	-22(12)
6	-5(4)	1.3(3)	-0.2(1)	-4(4)
7	-1.4(13)	0.20(6)	-0.016(1)	-1.3(13)

TABLE III. The fourth virial coefficient of  $^3\text{He}$  and its contributions.  $D_{xc}$  is defined in Eq. (32) and the other quantities are as in Table I. The expanded uncertainty in the last column is at  $k = 2$  coverage.

Temperature (K)	$D_{\text{Boltz}}(T)$ (cm $^9$ mol $^{-3}$ )	$D_{xc}(T)$ (cm $^9$ mol $^{-3}$ )	$u_V(D)$ (cm $^9$ mol $^{-3}$ )	$u_4(D)$ (cm $^9$ mol $^{-3}$ )	$D(T)$ (cm $^9$ mol $^{-3}$ )	$U(D)$ (cm $^9$ mol $^{-3}$ )
2.6	55000(15000)	20600(2200)	9000	1300	75000	30000
3	35000(9000)	5100(1300)	4000	500	40000	19000
4	22600(3000)	900(500)	1300	160	23500	7000
5	14100(1500)	170(50)	1400	90	14300	4000
6	8900(900)	60(30)	600	70	8900	2000
7	7000(500)	10(8)	300	60	7000	1300
8	5900(400)	1(2)	200	50	5900	900
10	5020(180)	0.0(3)	100	40	5020	400
15	3790(90)		30	30	3790	190
20	3540(30)		16	20	3535	80
30	3130(12)		7	14	3128	40
50	2483(4)		2	9	2483	20
80	1890.6(14)		1.2	6	1891	13
120	1437.6(7)		0.8	4	1438	9
200	979.2(3)		0.6	3	979	6
250	816.5(3)		0.5	2	817	5
273.16	757.6(3)		0.5	2	758	5
300	699.3(3)		0.5	2	699	4
400	541.1(2)		0.5	2	541	4
500	438.61(17)		0.4	2	439	4
700	313.22(16)		0.4	1.9	313	4
1000	212.84(15)		0.4	1.9	213	4
1500	130.88(5)		0.3	1.8	131	4
2000	89.41(4)		0.3	1.6	89	3

### C. Low-temperature behavior

Since one of the novel features of this work is the incorporation of exchange effects that become important at low temperature, in Figs. 2 and 3 we show low-temperature results for  $^4\text{He}$  and  $^3\text{He}$ , respectively. No low-temperature experimental data are available for comparison in either case.

In Fig. 2, we see that  $D(T)$  for  $^4\text{He}$  goes through a maximum near 4.5 K, turning sharply negative at the lowest tem-

peratures (the three lowest temperatures in Table I are not plotted; they would be far below the bottom of the graph). We do not show the effect of exchange, since as discussed above the exchange contributions are relatively small compared to their uncertainty due to terms of opposite sign. The correlation that Schultz and Kofke<sup>15</sup> fitted to their Boltzmann results is in excellent agreement with the results obtained here down to its lower temperature limit of 20 K. It extrapolates well down to 15 K, but becomes increasingly inaccurate when extrapolated

TABLE IV. The exchange contributions to  $D(T)$  for  ${}^3\text{He}$ , see Eqs. (30)–(37). Uncertainties here are  $k = 1$ .

Temperature (K)	$D_{01}(T)$ (cm $^9$ mol $^{-3}$ )	$D_{e1}(T)$ (cm $^9$ mol $^{-3}$ )	$D_{02}(T)$ (cm $^9$ mol $^{-3}$ )	$D_{xc}(T)$ (cm $^9$ mol $^{-3}$ )
2.6	-22257(2985)	27603(896)	-20809(51)	20631(2158)
3	-3185(1759)	10980(328)	-6263(15)	5120(1255)
4	-1044(692)	1281(42)	-414.4(13)	894(490)
5	-230(75)	197(8)	-38(2)	169(53)
6	-93(40)	39(2)	-4.35(3)	57(28)
7	-17(12)	8(5)	-0.602(7)	10(8)
8	-0.3(34)	1.6(1)	-0.091(2)	0.6(24)
10	0.0(4)	0.02(1)	-0.003(3)	0.02(27)

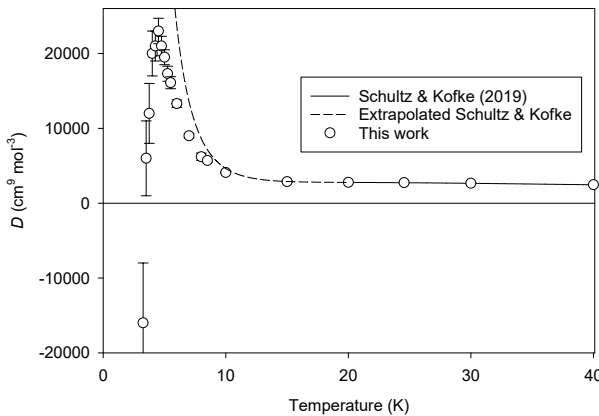


FIG. 2. Calculated values of  $D(T)$  for  ${}^4\text{He}$  at low temperatures. The correlation fitted to first-principles calculations by Schultz and Kofke<sup>15</sup> is extrapolated below 20 K. Error bars represent expanded uncertainties with coverage factor  $k = 2$ , and are smaller than the symbol size at higher temperatures.

further.

Figure 3 shows the low-temperature results for  ${}^3\text{He}$ . No maximum is evident in the temperature range investigated. We also show the values of  $D(T)$  obtained when only Boltzmann statistics are considered. Incorporation of exchange effects is necessary for quantitative accuracy below roughly 4 K. The significant exchange effects on  $D(T)$  for  ${}^3\text{He}$ , compared to a smaller effect for  ${}^4\text{He}$  due to competing terms, is similar to the behavior found in our previous work for  $C(T)$ .<sup>9,10</sup>

## VI. CONCLUSIONS

The values of  $D(T)$  presented in Table I (for  ${}^4\text{He}$ ) and Table III (for  ${}^3\text{He}$ ) represent the first such values calculated from the current state-of-the-art pair and three-body potentials. They are also the first to include exchange effects, and the first to include complete uncertainty estimates. For  ${}^3\text{He}$ , Table III presents the first fully quantum calculations of  $D(T)$ .

Our  ${}^4\text{He}$  calculations at the level of Boltzmann statistics confirm previous calculations (with a slightly different two-

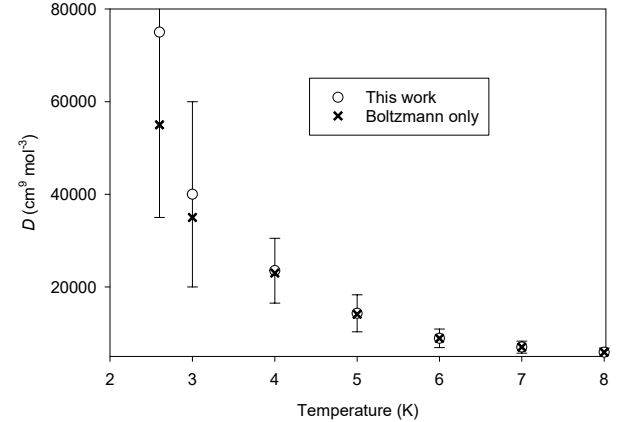


FIG. 3. Calculated values of  $D(T)$  for  ${}^3\text{He}$  at low temperatures, also showing results from Boltzmann statistics alone. Error bars represent expanded uncertainties with coverage factor  $k = 2$ .

body potential) from the group of Kofke.<sup>14,15</sup> Because the two-body potential used in that work<sup>5</sup> differs negligibly from the current state of the art for the purpose of calculating  $D(T)$ , we could consider those calculations to be additional data that supplement ours, making use of their somewhat smaller statistical uncertainties to improve our estimates of the Boltzmann contributions.

The exchange contributions to  $D$  for  ${}^4\text{He}$  are relatively small, due to terms of opposite sign that mostly cancel each other. Because of this cancellation, our statistical uncertainty for the exchange contribution is similar in magnitude to the contribution itself. In contrast, for the fermion  ${}^3\text{He}$ , the exchange contributions all contribute in the positive direction, producing a significant effect on  $D(T)$  at temperatures of roughly 4 K and below.

Several factors contribute to the uncertainty of the results. At low temperatures, the statistical uncertainty of the PIMC calculations is significant, not only in its own right but also in its contribution to the uncertainty  $u_V(D)$  due to the uncertainty in the potential, which at the lowest temperatures is estimated by taking differences between PIMC calculations with shifted potentials. This could be somewhat improved with more computer resources, and also by employing some of the optimized

methods for integrating virial coefficients developed by the group of Kofke.<sup>14,15</sup>

Uncertainty due to imperfect knowledge of the potential cannot be reduced simply with more computer time; this aspect, which dominates the uncertainty at higher temperatures, requires careful development of potential-energy surfaces. The pair potential is now known with extraordinary accuracy;<sup>7</sup> further improvement may be desirable for other reasons but it will not reduce the uncertainty of virial coefficients beyond  $B(T)$ . The three-body potential has an estimated expanded ( $k = 2$ ) uncertainty of 2% at all configurations,<sup>13</sup> which could be reduced somewhat with a concerted effort. Finally, the four-body potential is unknown, and is the largest uncertainty above roughly 10 K. Even an approximate four-body nonadditive potential, for example with a 20% uncertainty, would have a large impact on reducing the uncertainty of  $D(T)$ . The most important aspect of such a surface for metrology near room temperature would be its behavior at short-distance configurations dominated by repulsion, since those are the most important configurations at those temperatures. For use at cryogenic temperatures where the four-body uncertainty is still significant but the dispersion contribution is likely more important, its long-range behavior should approach that derived by Bade.<sup>29</sup>

## ACKNOWLEDGMENTS

The authors thank David Kofke and Andrew Schultz of the University at Buffalo for useful discussions on the calculation of the Boltzmann part of  $D(T)$ , Mark McLinden of NIST for insight into the experiments reported in Refs. 39 and 40, and Dan Friend for suggestions that improved clarity.

G.G. acknowledges support from *Real-K* project 18SIB02, which has received funding from the EMPIR programme co-financed by the Participating States and from the European Union's Horizon 2020 research and innovation programme.

The calculations for  $T \geq 20$  K have been performed on the computing cluster KORE at Fondazione Bruno Kessler. We acknowledge the CINECA award IscraC-FAVOHLA under the ISCRA initiative, for the availability of high performance computing resources and support.

## DATA AVAILABILITY

The data that support the findings of this study are available within this article.

<sup>1</sup>M. R. Moldover, R. M. Gavioso, J. B. Mehl, L. Pitre, M. de Podesta, and J. T. Zhang, "Acoustic gas thermometry," *Metrologia* **51**, R1–R19 (2014).

<sup>2</sup>C. Gaiser, T. Zandt, and B. Fellmuth, "Dielectric-constant gas thermometry," *Metrologia* **52**, S217–S226 (2015).

<sup>3</sup>P. M. C. Rourke, C. Gaiser, B. Gao, D. M. Ripa, M. R. Moldover, L. Pitre, and R. J. Underwood, "Refractive-index gas thermometry," *Metrologia* **56**, 032001 (2019).

<sup>4</sup>C. Gaiser, B. Fellmuth, and W. Sabuga, "Primary gas-pressure standard from electrical measurements and thermophysical ab initio calculations," *Nature Phys.* **16**, 177–180 (2020).

<sup>5</sup>W. Cencek, M. Przybytek, J. Komasa, J. B. Mehl, B. Jeziorski, and K. Szalewicz, "Effects of adiabatic, relativistic, and quantum electrodynamics interactions on the pair potential and thermophysical properties of helium," *J. Chem. Phys.* **136**, 224303 (2012).

<sup>6</sup>M. Przybytek, W. Cencek, B. Jeziorski, and K. Szalewicz, "Pair potential with submillikelvin uncertainties and nonadiabatic treatment of the halo state of the helium dimer," *Phys. Rev. Lett.* **119**, 123401 (2017).

<sup>7</sup>P. Czachorowski, M. Przybytek, M. Lesiuk, M. Puchalski, and B. Jeziorski, "Second virial coefficients for  ${}^4\text{He}$  and  ${}^3\text{He}$  from an accurate relativistic interaction potential," *Phys. Rev. A* **102**, 042810 (2020).

<sup>8</sup>J. O. Hirschfelder, C. F. Curtiss, and R. B. Bird, *Molecular Theory of Gases and Liquids* (John Wiley & Sons, New York, 1954).

<sup>9</sup>G. Garberoglio and A. H. Harvey, "Path-integral calculation of the third virial coefficient of quantum gases at low temperatures," *J. Chem. Phys.* **134**, 134106 (2011).

<sup>10</sup>G. Garberoglio and A. H. Harvey, "Erratum: Path-integral calculation of the third virial coefficient of quantum gases at low temperatures," *J. Chem. Phys.* **152**, 199903 (2020).

<sup>11</sup>G. Garberoglio, M. R. Moldover, and A. H. Harvey, "Improved first-principles calculation of the third virial coefficient of helium," *J. Res. Natl. Inst. Stand. Technol.* **116**, 729–742 (2011).

<sup>12</sup>G. Garberoglio, M. R. Moldover, and A. H. Harvey, "Erratum: Improved first-principles calculation of the third virial coefficient of helium," *J. Res. Natl. Inst. Stand. Technol.* **125**, 125019 (2020).

<sup>13</sup>W. Cencek, K. Patkowski, and K. Szalewicz, "Full-configuration-interaction calculation of three-body nonadditive contribution to helium interaction potential," *J. Chem. Phys.* **131**, 064105 (2009).

<sup>14</sup>K. R. S. Shaul, A. J. Schultz, and D. A. Kofke, "Path-integral Mayer-sampling calculations of the quantum Boltzmann contribution to virial coefficients of helium-4," *J. Chem. Phys.* **137**, 184101 (2012).

<sup>15</sup>A. J. Schultz and D. A. Kofke, "Virial coefficients of helium-4 from *ab initio*-based molecular models," *J. Chem. Eng. Data* **64**, 3742–3754 (2019).

<sup>16</sup>B. Gao, H. Zhang, D. Han, C. Pan, H. Chen, Y. Song, W. Liu, J. Hu, X. Kong, F. Sparasci, M. Plimmer, E. Luo, and L. Pitre, "Measurement of thermodynamic temperature between 5 K and 24.5 K with single-pressure refractive-index gas thermometry," *Metrologia* **57**, 065006 (2020).

<sup>17</sup>G. Garberoglio, "Quantum effects on virial coefficients: a numerical approach using centroids," *Chem. Phys. Lett.* **525–526**, 19–23 (2012).

<sup>18</sup>T. L. Hill, *An Introduction to Statistical Thermodynamics* (Dover, New York, 1987).

<sup>19</sup>T. L. Hill, *Statistical Mechanics* (Dover, New York, 1987).

<sup>20</sup>M. E. Boyd, S. Y. Larsen, and J. E. Kilpatrick, "Quantum mechanical second virial coefficient of a Lennard-Jones gas. Helium," *J. Chem. Phys.* **50**, 4034–4055 (1969).

<sup>21</sup>G. Lepage, "VEGAS: An adaptive multi-dimensional integration program," *Tech. Rep. (Cornell preprint CLNS 80-447, 1980)*.

<sup>22</sup>R. Kreckel, "Parallelization of adaptive MC integrators," *Comput. Phys. Commun.* **106**, 258–266 (1997).

<sup>23</sup>P. Levy, *Memorial des Sciences Mathématiques* (Gauthier Villars, Paris, 1954) fascicule 126.

<sup>24</sup>H. F. Jordan and L. D. Fosdick, "Three-particle effects in the pair distribution function for  $\text{He}^4$  gas," *Phys. Rev.* **171**, 128–149 (1968).

<sup>25</sup>R. Rodríguez-Cantano, R. Pérez de Tudela, M. Bartolomei, M. I. Hernández, J. Campos-Martínez, T. González-Lezana, P. Villarreal, J. Hernández-Rojas, and J. Bretón, "Examination of the Feynman–Hibbs approach in the study of NeN-coronene clusters at low temperatures," *J. Phys. Chem. A* **120**, 5370–5379 (2016).

<sup>26</sup>G. Garberoglio and A. H. Harvey, "First-principles calculation of the third virial coefficient of helium," *J. Res. Natl. Inst. Stand. Technol.* **114**, 249–262 (2009).

<sup>27</sup>W. Cencek, G. Garberoglio, A. H. Harvey, M. O. McLinden, and K. Szalewicz, "Three-body nonadditive potential for argon with estimated uncertainties and third virial coefficient," *J. Phys. Chem. A* **117**, 7542–7552 (2013).

<sup>28</sup>W. L. Bade, "Drude-model calculation of dispersion forces. I. General theory," *J. Chem. Phys.* **27**, 1280–1284 (1957).

<sup>29</sup>W. L. Bade, "Drude-model calculation of dispersion forces. III. The fourth-order contribution," *J. Chem. Phys.* **28**, 282–284 (1958).

<sup>30</sup>J. Wiebke, E. Pahl, and P. Schwerdtfeger, "Up to fourth virial coefficients from simple and efficient internal-coordinate sampling: Application

to neon,” *J. Chem. Phys.* **137**, 014508 (2012).

<sup>31</sup>J. Wiebke, E. Pahl, and P. Schwerdtfeger, “Sensitivity of the thermal and acoustic virial coefficients of argon to the argon interaction potential,” *J. Chem. Phys.* **137**, 064702 (2012).

<sup>32</sup>C. Gaiser and B. Fellmuth, “Polarizability of helium, neon, and argon: New perspectives for gas metrology,” *Phys. Rev. Lett.* **120**, 123203 (2018).

<sup>33</sup>M. Puchalski, K. Szalewicz, M. Lesiuk, and B. Jeziorski, “QED calculation of the dipole polarizability of helium atom,” *Phys. Rev. A* **101**, 022505 (2020).

<sup>34</sup>A. J. Thakkar, “The generator coordinate method applied to variational perturbation theory. Multipole polarizabilities, spectral sums, and dispersion coefficients for helium,” *J. Chem. Phys.* **75**, 4496–4501 (1981).

<sup>35</sup>A. L. Blancett, K. R. Hall, and F. B. Canfield, “Isotherms for the He–Ar system at 50°C, 0°C and -50°C up to 700 atm,” *Physica* **47**, 75–91 (1970).

<sup>36</sup>K. R. Hall and F. B. Canfield, “A least-squares method for reduction of Burnett data to compressibility factors and virial coefficients,” *Physica* **47**, 99–108 (1970).

<sup>37</sup>K. R. Hall and F. B. Canfield, “Isotherms for the He–N<sub>2</sub> system at -190°C, -170°C and -160°C up to 700 atm,” *Physica* **47**, 219–226 (1970).

<sup>38</sup>J. A. Provine and F. B. Canfield, “Isotherms for the He–Ar system at -130, -115, and -90°C up to 700 atm,” *Physica* **52**, 79–91 (1971).

<sup>39</sup>M. O. McLinden and C. Lösch-Will, “Apparatus for wide-ranging, high-accuracy fluid ( $p, \rho, T$ ) measurements based on a compact two-sinker densimeter,” *J. Chem. Thermodyn.* **39**, 507–530 (2007).

<sup>40</sup>M. R. Moldover and M. O. McLinden, “Using *ab initio* “data” to accurately determine the fourth density virial coefficient of helium,” *J. Chem. Thermodyn.* **42**, 1193–1203 (2010).

<sup>41</sup>M. O. McLinden, National Institute of Standards and Technology, personal communication (2020).